# A New Adaptive-Robust Design for Time Delay Control under State-Dependent Stability Condition

Roy, Spandan; Lee, Jinoh; Baldi, Simone

**DOI**
10.1109/TCST.2020.2969129

**Publication date**
2021

**Document Version**
Accepted author manuscript

**Published in**
IEEE Transactions on Control Systems Technology

**Citation (APA)**
Roy, S., Lee, J., & Baldi, S. (2021). A New Adaptive-Robust Design for Time Delay Control under State-Dependent Stability Condition. *IEEE Transactions on Control Systems Technology*, *29*(1), 420-427. https://doi.org/10.1109/TCST.2020.2969129

# A New Adaptive-Robust Design for Time Delay Control under State-dependent Stability Condition

Spandan Roy, *Member, IEEE*, Jinoh Lee, *Senior Member, IEEE*, and Simone Baldi, *Senior Member, IEEE*

***Abstract*—This paper proposes a new adaptive-robust formulation for time-delay control (TDC) under a less restrictive stability condition. TDC relies on estimating the unknown system dynamics via the artificial introduction of a time delay, often referred to as time-delay estimation (TDE). In conventional TDC, the estimation error, called TDE error, is taken to be upper-bounded by a constant under the assumption of small time delay and, most importantly, of a priori bounded states. We highlight the issues of such conventional methodology via an unstable counterexample. Consequently, a new less restrictive structure for the upper bound of the TDE error is formulated, which has an explicit dependency on system states and is valid for any chosen time delay. This insight leads to a new TDC design, namely time-delayed adaptive-robust control (TDARC). The effectiveness of TDARC is substantiated via a multiple-degrees-of-freedom robot.**

***Index Terms*—Adaptive-robust control, Euler-Lagrange systems, state-dependent uncertainty, time-delay control.**

## I. Introduction

THE erstwhile *time-delay control* (TDC) was conceptualized in parallel by [1], [2] and [3] as an alternate control scheme that requires neither structural knowledge of the system like conventional adaptive control nor bound of the uncertainties like conventional robust control. TDC is based on the *time-delay estimation* (TDE) method, wherein a delay is artificially (i.e., intentionally) introduced to estimate unknown system dynamics using the state/input data collected at the immediate previous time instant [1]–[3].

The simplicity and effectiveness of TDC in practical scenarios have led to its applications in various domains in the past two and half decades, such as unmanned vehicles [4]–[7], shape memory alloys [8], [9], different types of actuators [10], [11], manipulators [12]–[14], humanoids [15], [16], fuel-cell systems [17], and synchronous motors [18]. It has been shown that TDC can provide better performance over PID control [5], [10] or over a class of adaptive sliding mode control [4]. However, the unattended estimation error stemming from the estimation process in TDC, commonly termed as the *TDE error*, causes detrimental effect to the performance of TDC. To counteract this problem, a few notable works have been reported in literature such as internal model [19], ideal velocity feedback [13], [20], gradient estimator [21], conventional sliding mode control [7], [22] and the recently developed adaptive switching gain control [6], [23], [24].

An important condition for any TDC-based method is the boundedness of the TDE error. All the existing TDC designs [4]–[24] are built in continuous-time domain upon the boundedness condition derived in [1]–[3]. However, this condition is found to be conservative based on the following grounds:

- It is derived assuming small sampling interval (acting as the artificially introduced time delay), which is not always possible.
- During the derivation procedures, a function which explicitly depends on system states, is considered to be upper bounded by a constant; such restrictive consideration imposes the states to be bounded a priori.

These fundamental issues of the conventional TDC [1]–[24] form the core motivation and two major contributions of this paper. First, as compared to existing structures [1]–[24], a generalized structure of the TDE error is formulated which can handle possibly non-small delays and has explicit dependence on the system states (no a priori bounded states are required). Second, unlike conventional TDC designs [1]–[24], the state-dependent structure cannot guarantee stability leaving the TDE error uncompensated. Therefore, a novel TDC framework, christened as time-delayed adaptive-robust control (TDARC), is formulated to compensate for the TDE error without any prior knowledge of the uncertain system dynamics.

The rest of the paper is organized as follows: In Section II, the design issues of a conventional TDC are clarified. Section III details the proposed TDARC with stability analysis in Section IV. Section V presents comparative performance evaluations of TDARC. Section VI concludes the work.

The following notations are used in the paper: $(\bullet)_L$ denotes that $(\bullet)(t)$ is delayed by $L$, i.e., $(\bullet)(t-L)$; $\lambda_{\min}(\bullet)$, $\lambda_{\max}(\bullet)$, $||\bullet||$, $|\bullet|$ denote minimum and maximum eigenvalue, 2-norm and absolute value of $\bullet$ respectively; $\mathbf{I}$ denotes Identity matrix.

Manuscript received August 8, 2019; revised November 20, 2019; accepted January 15, 2020. *(Corresponding authors: Jinoh Lee and Simone Baldi.)*

This work was supported in part by the "Fundamental Research Funds for The Central Universities" under Grant 4007019109 and in part by the Special Guiding Funds for "Double First-Class" under Grant 4007019201.

S. Roy is with Robotics Research Center, International Institute of Information Technology Hyderabad (IIIT-H), Hyderabad, India and was with Delft Center for Systems and Control (DCSC), Technische Universiteit Delft (TU Delft), Delft, The Netherlands e-mail: (spandan.roy@iiit.ac.in).

J. Lee is with the Advanced Robotics Department, Fondazione Istituto Italiano di Tecnologia (IIT), Genoa, Italy e-mail: (jinoh.lee@iit.it).

S. Baldi is with the School of Mathematics, Southeast University, Nanjing, China and with DCSC, TU Delft, Delft, The Netherlands (e-mail: s.baldi@tudelft.nl).

Color versions of one or more of the figures in this article are available online at http://ieeexplore.ieee.org.

Digital Object Identifier 00.0000/TCST.2020.0000

## II. Time-Delay Control: Formulation and Issues

The purpose of this section is to briefly discuss the basic ideas of the TDC and outline the motivations behind this work.

Let us base the discussion on the following class of Euler-Lagrange (EL) systems, widely adopted in TDC [1]–[24]

$$\mathbf{M}(\mathbf{q})\ddot{\mathbf{q}} + \mathbf{H}(\mathbf{q}, \dot{\mathbf{q}}) = \boldsymbol{\tau}, \tag{1}$$

where $\mathbf{q} \in \mathbb{R}^n$ is the system state, $\boldsymbol{\tau} \in \mathbb{R}^n$ is the generalized control input, $\mathbf{M}(\mathbf{q}) \in \mathbb{R}^{n\times n}$ is the mass/inertia matrix and $\mathbf{H}(\mathbf{q}, \dot{\mathbf{q}}) \in \mathbb{R}^n$ is the combination of other system dynamics terms (including unmodelled dynamics and disturbances).

The following property holds for EL systems and is exploited later in Section III-A for stability analysis.

**Property [25]:** The matrix $\mathbf{M}(\mathbf{q})$ is uniformly positive definite for all $\mathbf{q}$, i.e., $\exists \psi_1, \psi_2 \in \mathbb{R}^+$ such that

$$\psi_1 \mathbf{I} \leq \mathbf{M}(\mathbf{q}) \leq \psi_2 \mathbf{I} \Rightarrow (1/\psi_2)\mathbf{I} \leq \mathbf{M}^{-1}(\mathbf{q}) \leq (1/\psi_1)\mathbf{I} \tag{2}$$

Introducing a constant diagonal matrix $\bar{\mathbf{M}}$, one can obtain

$$\bar{\mathbf{M}}\ddot{\mathbf{q}} + \mathbf{N}(\mathbf{q}, \dot{\mathbf{q}}, \ddot{\mathbf{q}}) = \boldsymbol{\tau}, \tag{3}$$

$$\text{with} \quad \mathbf{N}(\mathbf{q}, \dot{\mathbf{q}}, \ddot{\mathbf{q}}) = [\mathbf{M}(\mathbf{q}) - \bar{\mathbf{M}}]\ddot{\mathbf{q}} + \mathbf{H}(\mathbf{q}, \dot{\mathbf{q}}). \tag{4}$$

Let us decompose the control input $\boldsymbol{\tau}$ as

$$\boldsymbol{\tau} = \bar{\mathbf{M}}\mathbf{u}_0 + \hat{\mathbf{N}}(\mathbf{q}, \dot{\mathbf{q}}, \ddot{\mathbf{q}}), \tag{5}$$

where $\mathbf{u}_0$ is the auxiliary control input, and $\hat{\mathbf{N}}$ is the estimated value of $\mathbf{N}$ to be designed. TDC was originally proposed in [1]–[3] with the main aim to reduce the modelling effort of (1) by approximating $\hat{\mathbf{N}}$ using the past input and state data as

$$\hat{\mathbf{N}}(\mathbf{q}, \dot{\mathbf{q}}, \ddot{\mathbf{q}}) \cong \mathbf{N}(\mathbf{q}_L, \dot{\mathbf{q}}_L, \ddot{\mathbf{q}}_L) = \boldsymbol{\tau}_L - \bar{\mathbf{M}}\ddot{\mathbf{q}}_L, \tag{6}$$

where $L > 0$ is a small time delay.

**Remark 1.** *System (1) is originally delay-free. The delay $L$ is artificially introduced to estimate the unknown dynamics term $\mathbf{N}$ as in (6). This estimation is conventionally called time-delay estimation (TDE). Hence, the terms TDE and TDC are not to be associated with the process of estimating any time-delay.*

The control objective is to track a desired trajectory $\mathbf{q}^d(t)$, designed such that $\mathbf{q}^d, \dot{\mathbf{q}}^d, \ddot{\mathbf{q}}^d \in \mathcal{L}_\infty$. Defining the tracking error as $\mathbf{e}(t) = \mathbf{q}^d(t) - \mathbf{q}(t)$, the auxiliary control input $\mathbf{u}_0$ in (13) is designed as

$$\mathbf{u}_0 = \ddot{\mathbf{q}}^d + \mathbf{K}_D\dot{\mathbf{e}} + \mathbf{K}_P\mathbf{e}, \tag{7}$$

where $\mathbf{K}_P, \mathbf{K}_D \in \mathbb{R}^{n\times n}$ are two positive definite matrices.

Substituting (5) in (3), following error dynamics is obtained:

$$\ddot{\mathbf{e}} = -\mathbf{K}_D\dot{\mathbf{e}}_L - \mathbf{K}_P\mathbf{e}_L + \boldsymbol{\sigma}, \tag{8}$$

where $\boldsymbol{\sigma} = \bar{\mathbf{M}}^{-1}(\mathbf{N} - \hat{\mathbf{N}})$ represents the *estimation error stemming from (6)*. In the following, variable dependency will be omitted whenever obvious.

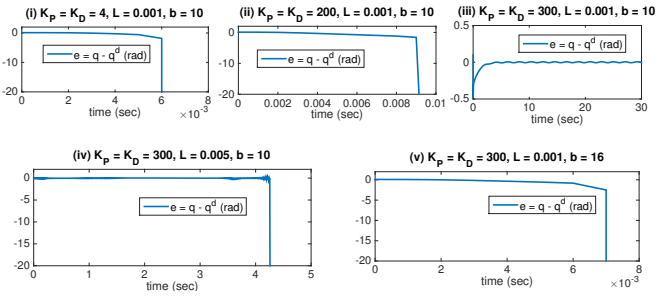


Fig. 1. Tracking error with the conventional TDC for system (12).

### A. A priori conditions in conventional TDC

After some mathematical arrangements, as detailed in [1]–[4], the structure of $\boldsymbol{\sigma}$ is evaluated as

$$\boldsymbol{\sigma} = \mathbf{E}\boldsymbol{\sigma}_L + \boldsymbol{\Phi}_1 - \mathbf{E}\boldsymbol{\Phi}_2, \tag{9}$$

where $\boldsymbol{\Phi}_1 \triangleq \mathbf{M}^{-1}\{(\mathbf{M}_L - \mathbf{M})\ddot{\mathbf{q}}_L + \mathbf{N}_L - \mathbf{N}\}$, $\boldsymbol{\Phi}_2 \triangleq (\mathbf{u}_0)_L - \mathbf{u}_0$, and $\mathbf{E} \triangleq (\mathbf{I} - \mathbf{M}^{-1}(\mathbf{q})\bar{\mathbf{M}})$. Assuming $L$ is selected small enough so that the discretization error can be neglected, and *assuming that* $|\boldsymbol{\Phi}_{1i}| < \rho_1$, $|\boldsymbol{\Phi}_{2i}| < \rho_2$, $i = 1, \cdots, n$, the conventional TDC ([1]–[4]) derives the following upper bound of $\boldsymbol{\sigma}$ in the discrete-time domain:

$$\lim_{k\to\infty} ||\boldsymbol{\sigma}(k)|| \leq \frac{n(\rho_1 + \lambda_{\max}(\mathbf{E}(k))\rho_2)}{1 - \lambda_{\max}(\mathbf{E}(k))} \tag{10}$$

where $\bar{\mathbf{M}}$ is selected such that the following condition holds:

$$|\lambda_{\max}(\mathbf{E}(k))| < 1. \tag{11}$$

**Remark 2.** *Two sources of conservativeness involved in the conventional upper bound structure (9)-(10) are listed:*

1. *The condition (10) is derived based on the assumption that the sampling interval $L$ is small enough to ignore the discretization error. Handling the case in which the discretization error cannot be ignored is open.*
2. *Assuming the upper bounds of $\boldsymbol{\Phi}_1, \boldsymbol{\Phi}_2$ in (9) to be constant is restrictive in nature due to their explicit dependence on the system states, i.e., it imposes the states to be bounded a priori [26].*

### B. An Unstable Counterexample

To illustrate the consequences of Remark 2, we consider an academic example

$$m\ddot{q} + b\dot{q}^2|q| + kq = \tau, \tag{12}$$

which is required to follow $q^d = \sin(3t)$. Let us apply TDC (5)-(7) with $m = 2 + 0.5\sin(t), \overline{m} = 2, k = 10, q(0) = 0.1$ under five different parametric scenarios of $K_D, K_P, L$ and $b$ as shown in Fig. 1. For all scenarios, (11) is satisfied. For system (12), we have via (4), (7) and (9) state-dependent $\boldsymbol{\Phi}_1 = (m - \overline{m})(\ddot{q}_L - \ddot{q}) + b((\dot{q}^2|q|)_L - \dot{q}^2|q|) + k(q_L - q)$, $\boldsymbol{\Phi}_2 = (\ddot{q}^d_L - \ddot{q}^d) + K_D(\dot{e}_L - \dot{e}) + K_P(e_L - e)$ , which clearly cannot be bounded a priori. The state responses for $L = 0.001$ in scenarios (i), (ii) and (iii) reveal stability only for *sufficiently large* $K_P, K_D$. Even for large $K_P, K_D$, one can still find a sufficiently large $L$ as in scenario (iv) or a sufficiently large $b$

as in scenario (v) for which instability reappears. Therefore, the situation is the following: the conventional TDC requires $\mathbf{\Phi}_1$ and $\mathbf{\Phi}_2$ to be bounded a priori; however, when $\mathbf{\Phi}_1$ and $\mathbf{\Phi}_2$ are state-dependent, such a priori boundedness is lost, allowing us to find many instability examples.

Noting that state-dependent uncertainty naturally occurs in many mechatronic systems (cf. [26], [27]), in the following we will formulate a novel TDC framework without any a priori boundedness assumption.

## III. Time-Delayed Adaptive-Robust Framework

The control input $\boldsymbol{\tau}$ of the proposed TDARC is designed to have a similar structure like (5) with modified $\mathbf{u}$ as

$$\mathbf{u} = \mathbf{u}_0 + \mathbf{\Delta u}, \tag{13}$$

where $\mathbf{u}_0$ as in (7) and $\mathbf{\Delta u}$ being the adaptive-robust control part of TDARC designed as

$$\mathbf{\Delta u}(t) = \alpha c \ \text{sig}(\mathbf{s}, \epsilon), \tag{14}$$

where $\mathbf{s} = \mathbf{B}^T\mathbf{P}\boldsymbol{\xi}$, $\boldsymbol{\xi} = \begin{bmatrix}\mathbf{e}^T & \dot{\mathbf{e}}^T\end{bmatrix}^T$ and $\mathbf{P} > \mathbf{0}$ is the solution of the Lyapunov equation $\mathbf{A}^T\mathbf{P} + \mathbf{PA} = -\mathbf{Q}$ for some $\mathbf{Q} > \mathbf{0}$, where $\mathbf{A} = \begin{bmatrix}\mathbf{0} & \mathbf{I} \\ -\mathbf{K}_P & -\mathbf{K}_D\end{bmatrix}$, $\mathbf{B} = \begin{bmatrix}\mathbf{0} \\ \mathbf{I}\end{bmatrix}$; $\alpha \in \mathbb{R}^+$ is a user-defined scalar; $c \in \mathbb{R}^+$ is the overall switching gain which provides robustness against the TDE error (the structure of $c$ will be defined in subsection III-B); and $\text{sig}(\mathbf{s}, \epsilon)$ is a sigmoid function defined as $\text{sig}(\mathbf{s}, \epsilon) \triangleq \mathbf{s}/\sqrt{||\mathbf{s}||^2 + \epsilon}$. Here, $\epsilon$ is a small positive scalar used to avoid chattering. Substituting (5) and (7)-(14) into (1) gives the following error dynamics:

$$\ddot{\mathbf{e}} = -\mathbf{K}_D\dot{\mathbf{e}} - \mathbf{K}_P\mathbf{e} + \boldsymbol{\sigma} - \mathbf{\Delta u} \tag{15}$$

$$\Rightarrow \dot{\boldsymbol{\xi}} = \mathbf{A}\boldsymbol{\xi} + \mathbf{B}(\boldsymbol{\sigma} - \mathbf{\Delta u}). \tag{16}$$

Positive definiteness of $\mathbf{K}_P$ and $\mathbf{K}_D$ guarantees that $\mathbf{A}$ is Hurwitz. Finally, combining (5), (6), (13)-(14), TDARC becomes

$$\begin{aligned}\boldsymbol{\tau} = \underbrace{\boldsymbol{\tau}_L - \bar{\mathbf{M}}\ddot{\mathbf{q}}_L}_{\text{TDE part}} + \underbrace{\bar{\mathbf{M}}(\ddot{\mathbf{q}}^d + \mathbf{K}_D\dot{\mathbf{e}} + \mathbf{K}_P\mathbf{e})}_{\text{Desired dynamics injection part}} \\ + \quad \underbrace{\alpha\bar{\mathbf{M}}c\text{sig}(\mathbf{s}, \epsilon)}_{\text{Adaptive-robust control part}}.\end{aligned} \tag{17}$$

The rationale behind the introduction of the adaptive-robust term is detailed in subsection III-B.

### A. New upper bound structure of $\boldsymbol{\sigma}$

A new structure on $||\boldsymbol{\sigma}||$ is here formulated. From (4) and (15), the following two relations can be achieved:

$$\hat{\mathbf{N}} = \mathbf{N}_L = [\mathbf{M}(\mathbf{q}_L) - \bar{\mathbf{M}}]\ddot{\mathbf{q}}_L + \mathbf{H}_L, \tag{18}$$

$$\boldsymbol{\sigma} = \ddot{\mathbf{q}} - \mathbf{u}. \tag{19}$$

Using (18), the control input $\boldsymbol{\tau}$ in (5) can be rewritten as

$$\boldsymbol{\tau} = \bar{\mathbf{M}}\mathbf{u} + [\mathbf{M}(\mathbf{q}_L) - \bar{\mathbf{M}}]\ddot{\mathbf{q}}_L + \mathbf{H}_L. \tag{20}$$

Multiplying both sides of (19) with $\mathbf{M}$ and using (1) and (20) we have

$$\begin{aligned}\mathbf{M}\boldsymbol{\sigma} &= \boldsymbol{\tau} - \mathbf{H} - \mathbf{Mu}, \\ &= \bar{\mathbf{M}}\mathbf{u} + [\mathbf{M}(\mathbf{q}_L) - \bar{\mathbf{M}}]\ddot{\mathbf{q}}_L + \mathbf{H}_L - \mathbf{H} - \mathbf{Mu}.\end{aligned} \tag{21}$$

Defining $\mathbf{K} \triangleq [\mathbf{K}_P \ \mathbf{K}_D]$ and using (15) we have

$$\ddot{\mathbf{q}}_L = \ddot{\mathbf{q}}_L^d - \ddot{\mathbf{e}}_L = \ddot{\mathbf{q}}_L^d + \mathbf{K}\boldsymbol{\xi}_L - \boldsymbol{\sigma}_L + \mathbf{\Delta u}_L. \tag{22}$$

Substituting (22) into (21), and after re-arrangement yields

$$\begin{aligned}\boldsymbol{\sigma} = &\underbrace{\mathbf{M}^{-1}\bar{\mathbf{M}}(\mathbf{\Delta u} - \mathbf{\Delta u}_L)}_{\boldsymbol{\chi}_1} + \underbrace{\mathbf{M}^{-1}(\mathbf{M}_L\mathbf{\Delta u}_L - \mathbf{M}\mathbf{\Delta u})}_{\boldsymbol{\chi}_2} \\ &+ \underbrace{\mathbf{M}^{-1}\{\bar{\mathbf{M}}\ddot{\mathbf{q}}^d - (\mathbf{M} - \mathbf{M}_L + \bar{\mathbf{M}})\ddot{\mathbf{q}}_L^d + \mathbf{H}_L - \mathbf{H}\}}_{\boldsymbol{\chi}_3} \\ &+ \underbrace{\mathbf{M}^{-1}(\mathbf{M}_L - \bar{\mathbf{M}})\mathbf{K}\boldsymbol{\xi}_L}_{\boldsymbol{\chi}_4} - \underbrace{\mathbf{M}^{-1}(\mathbf{M}_L - \bar{\mathbf{M}})\boldsymbol{\sigma}_L}_{\boldsymbol{\chi}_5} \\ &+ \underbrace{(\mathbf{M}^{-1}\bar{\mathbf{M}} - \mathbf{I})\mathbf{K}\boldsymbol{\xi}}_{\boldsymbol{\chi}_6}.\end{aligned} \tag{23}$$

Both $\mathbf{M}$ and $\mathbf{M}^{-1}$ are bounded from system property (2). Any function $\psi$ delayed by time $L$ can be represented as

$$\psi_L = \psi(t) - \int_{-L}^{0} \frac{\mathrm{d}}{\mathrm{d}\theta}\psi(t + \theta)\mathrm{d}\theta. \tag{24}$$

Integration of any continuous function or of any function with finite number of discontinuities (e.g., Coulumb friction) over a finite interval (here $-L$ to 0) is always finite [28]. Therefore, considering $\mathbf{\Delta u}$ as in (14) and using (24), the following conditions hold for unknown constants $\delta_i$, $i = 1, \cdots, 5$:

$$||\boldsymbol{\chi}_1|| = ||\mathbf{M}^{-1}\bar{\mathbf{M}}\int_{-L}^{0} \frac{\mathrm{d}}{\mathrm{d}\theta}\mathbf{\Delta u}(t + \theta)\mathrm{d}\theta|| \leq \delta_1 \tag{25}$$

$$||\boldsymbol{\chi}_2|| = ||-\mathbf{M}^{-1}\int_{-L}^{0} \frac{\mathrm{d}}{\mathrm{d}\theta}\mathbf{M}(t + \theta)\mathbf{\Delta u}(t + \theta)\mathrm{d}\theta|| \leq \delta_2 \tag{26}$$

$$\begin{aligned}||\boldsymbol{\chi}_3|| = ||\mathbf{M}^{-1}\{&\bar{\mathbf{M}}\ddot{\mathbf{q}}^d - (\mathbf{M} - \mathbf{M}_L + \bar{\mathbf{M}})\ddot{\mathbf{q}}_L^d \\ &- \int_{-L}^{0} \frac{\mathrm{d}}{\mathrm{d}\theta}\mathbf{H}(t + \theta)\mathrm{d}\theta\}|| \leq \delta_3\end{aligned} \tag{27}$$

$$\begin{aligned}||\boldsymbol{\chi}_4|| = ||\mathbf{M}^{-1}&\int_{-L}^{0} \frac{\mathrm{d}}{\mathrm{d}\theta}(\mathbf{M}(t + \theta) - \bar{\mathbf{M}})\mathbf{K}\boldsymbol{\xi}(t + \theta)\mathrm{d}\theta|| \\ &+ (\mathbf{M}^{-1}\bar{\mathbf{M}} - \mathbf{I})\mathbf{K}\boldsymbol{\xi}|| \leq ||\mathbf{EK}||||\boldsymbol{\xi}|| + \delta_4\end{aligned} \tag{28}$$

$$\begin{aligned}||\boldsymbol{\chi}_5|| &= ||\mathbf{E}\boldsymbol{\sigma} + \mathbf{M}^{-1}\int_{-L}^{0} \frac{\mathrm{d}}{\mathrm{d}\theta}\{(\mathbf{M}(t + \theta) - \bar{\mathbf{M}})\boldsymbol{\sigma}(t + \theta)\}\mathrm{d}\theta|| \\ &\leq ||\mathbf{E}||||\boldsymbol{\sigma}|| + \delta_5 \\ ||\boldsymbol{\chi}_6|| &= ||(\mathbf{M}^{-1}\bar{\mathbf{M}} - \mathbf{I})\mathbf{K}\boldsymbol{\xi}|| \leq ||\mathbf{EK}||||\boldsymbol{\xi}||.\end{aligned} \tag{29}$$

Here $\mathbf{M}$ and $\mathbf{H}$ are explicitly represented in time for ease of notation. Then, considering that the condition $||\mathbf{E}|| = ||\mathbf{I} - \mathbf{M}^{-1}(\mathbf{q})\bar{\mathbf{M}}|| < 1$ holds, the upper bound of $\boldsymbol{\sigma}$ is formulated using (25)-(29) from (23) as

$$\|\boldsymbol{\sigma}\| \leq \beta_0 + \beta_1\|\boldsymbol{\xi}\|, \tag{30}$$

$$\text{where } \beta_0 = \frac{\sum_{i=1}^{5}\delta_i}{1 - \|\mathbf{E}\|}, \ \beta_1 = \frac{2\|\mathbf{EK}\|}{1 - \|\mathbf{E}\|}. \tag{31}$$

**Remark 3.** *Let us highlight how the proposed upper bound structure of the TDE error $\boldsymbol{\sigma}$ in (30) addresses the conservative aspects of (10) mentioned in Remark 2.*

1. *In view of (24) and the argument below it, (30) is derived independently of the discretization error. Further, choice*

*of (how big or small) $L$ only affects the value of $\beta_0, \beta_1$ and not the structure (30).*

2. *It can be noted from (30) that the upper bound of $||\boldsymbol{\sigma}||$ preserves the explicit dependency on system states through $\boldsymbol{\xi}$. Thus, any prior restriction on the system states caused by the constant bound in (10) is eliminated.*

**Remark 4.** *An alternative state-dependent bound for $\boldsymbol{\sigma}$ was proposed in [29] consisting of seven parameters and using some knowledge of the various terms involved in $\mathbf{H}$ as in (1). In the following, we want to develop an adaptive controller exploiting the simpler two-parameter structure (30) without any a priori knowledge about such parameters. This direction is still unexplored to the best of the authors' knowledge.*

**Selection of the parameters $\beta_0$ and $\beta_1$:** Note that the two *positive gains* $\beta_0$ and $\beta_1$ are unknown, as $\|\mathbf{E}\| = \|\mathbf{I} - \mathbf{M}^{-1}(\mathbf{q})\bar{\mathbf{M}}\|$ is unknown, being $\mathbf{M}$ and $\mathbf{H}$ subject to uncertainty. One possibility is to design $\beta_0$ and $\beta_1$ in a robust control framework by utilizing an upper bound of $||\mathbf{E}|| < 1$. However, such worst-case design may lead to unnecessary high gain. Therefore, the adaptive-robust term in (17)) is appropriately designed to avoid any knowledge of $\beta_0$ and $\beta_1$.

### *B. Design of the Adaptive-Robust Law*

The switching gain $c$ in (14) is formulated based on the structure of $||\boldsymbol{\sigma}||$ as

$$c = \hat{\beta}_0 + \hat{\beta}_1||\boldsymbol{\xi}||, \tag{32}$$

where $\hat{\beta}_0, \hat{\beta}_1$ are the estimates of $\beta_0, \beta_1 \in \mathbb{R}^+$, respectively. The gains are evaluated as follows:

$$\dot{\hat{\beta}}_j = \begin{cases} \gamma_j \|\boldsymbol{\xi}\|^j \|\mathbf{s}\|, & \text{if any } \hat{\beta}_j \le \underline{\beta}_j \text{ or } \mathbf{s}^T\dot{\mathbf{s}} > 0 \\ -\gamma_j \|\boldsymbol{\xi}\|^j \|\mathbf{s}\|, & \text{if } \mathbf{s}^T\dot{\mathbf{s}} \le 0 \text{ and all } \hat{\beta}_j > \underline{\beta}_j \end{cases}, \tag{33}$$

with $\hat{\beta}_j(0) \ge \underline{\beta}_j$, where $\underline{\beta}_j \in \mathbb{R}^+$ $j = 0, 1$ are user-defined scalars. Using the first condition of (33) and the fact $\hat{\beta}_j(0) \ge \underline{\beta}_j$, it can be inferred that $\hat{\beta}_j(t) \ge \underline{\beta}_j$ $\forall t \ge 0$ $\forall j = 0, 1$. This condition is exploited later during the stability analysis.

## IV. Closed-Loop System Stability

The stability analysis of TDARC is carried out utilizing the following Lyapunov function candidate:

$$\bar{V} = V + (\hat{\beta}_0 - \beta_0^*)^2/(2\gamma_0) + (\hat{\beta}_1 - \beta_1^*)^2/(2\gamma_1), \tag{34}$$

where $V(\boldsymbol{\xi}) = (1/2)\boldsymbol{\xi}^T\mathbf{P}\boldsymbol{\xi}$ and $\beta_j^* \ge \beta_j(t) > 0$ is a constant. For the ease of analysis, we define a region such that

$$\alpha \frac{||\mathbf{s}||^2}{\sqrt{||\mathbf{s}||^2 + \epsilon}} \ge ||\mathbf{s}|| \Rightarrow ||\mathbf{s}|| \ge \sqrt{\frac{\epsilon}{\alpha^2 - 1}} \triangleq \varphi. \tag{35}$$

The condition (35) implies that one needs to select $\alpha > 1$, which is always possible since $\alpha$ is a user-defined scalar. The closed-loop system stability is stated in the following theorem:

**Theorem 1.** *The system (1) employing TDARC with the controller (17), (33) is Uniformly Ultimately Bounded (UUB).*

*Proof.* Exploring the various combinations of $\boldsymbol{\Delta}\mathbf{u}$, the gains $\hat{\beta}_j, j = 0, 1$ in (14), (33) and the condition (35), the stability of the overall system is analyzed for the following four possible cases using the common Lypaunov function (34):

**Case (i):** $||\mathbf{s}|| \ge \varphi$ and$\{$any $\hat{\beta}_j \le \underline{\beta}_j$ or $\mathbf{s}^T\dot{\mathbf{s}} > 0\}$
Using the Lyapunov equation $\mathbf{A}^T\mathbf{P} + \mathbf{P}\mathbf{A} = -\mathbf{Q}$, the time derivative of (34) yields

$$\begin{aligned} \dot{\bar{V}} &\le -(1/2)\boldsymbol{\xi}^T\mathbf{Q}\boldsymbol{\xi} + \mathbf{s}^T\{-\alpha c(\mathbf{s}/\sqrt{||\mathbf{s}||^2 + \epsilon}) + \boldsymbol{\sigma}\} \\ &\quad + ((\hat{\beta}_0 - \beta_0^*)/\gamma_0)\dot{\hat{\beta}}_0 + ((\hat{\beta}_1 - \beta_1^*)/\gamma_1)\dot{\hat{\beta}}_1 \\ &\le -(1/2)\boldsymbol{\xi}^T\mathbf{Q}\boldsymbol{\xi} - c||\mathbf{s}|| + (\beta_0^* + \beta_1^*||\boldsymbol{\xi}||)||\mathbf{s}|| \\ &\quad + (\hat{\beta}_0 - \beta_0^*)||\mathbf{s}|| + (\hat{\beta}_1 - \beta_1^*)||\boldsymbol{\xi}||||\mathbf{s}|| \\ &\le -(1/2)\lambda_{\min}(\mathbf{Q})||\boldsymbol{\xi}||^2 \le 0, \end{aligned} \tag{36}$$

as $\alpha > 1$. From (36) it can be inferred that $\bar{V}(t) \in \mathcal{L}_\infty$ implying $\boldsymbol{\xi}(t), \hat{\beta}_j(t) \in \mathcal{L}_\infty \Rightarrow \boldsymbol{\sigma}(t), \boldsymbol{\Delta}\mathbf{u} \in \mathcal{L}_\infty$ for Case (i).

**Case (ii):** $||\mathbf{s}|| \ge \varphi$ and $\{\mathbf{s}^T\dot{\mathbf{s}} \le 0$ and all $\hat{\beta}_j > \underline{\beta}_j\}$
For this case, the time derivative of (34) yields

$$\begin{aligned} \dot{\bar{V}} &\le -(1/2)\boldsymbol{\xi}^T\mathbf{Q}\boldsymbol{\xi} - c||\mathbf{s}|| + (\beta_0^* + \beta_1^*||\boldsymbol{\xi}||)||\mathbf{s}|| \\ &\quad - (\hat{\beta}_0 - \beta_0^*)||\mathbf{s}|| - (\hat{\beta}_1 - \beta_1^*)||\boldsymbol{\xi}||||\mathbf{s}|| \\ &\le -(1/2)\lambda_{\min}(\mathbf{Q})||\boldsymbol{\xi}||^2 + 2(\beta_0^* + \beta_1^*||\boldsymbol{\xi}||)||\mathbf{s}||. \end{aligned} \tag{37}$$

In this case we have $\mathbf{s}^T\dot{\mathbf{s}} \le 0$ which implies $||\mathbf{s}||, ||\boldsymbol{\xi}|| \in \mathcal{L}_\infty$ (cf. the relation $\mathbf{s} = \mathbf{B}^T\mathbf{P}\boldsymbol{\xi}$). Thus, $\exists \varsigma \in \mathbb{R}^+$ such that $2(\beta_0^* + \beta_1^*||\boldsymbol{\xi}||)||\mathbf{s}|| \le \varsigma$. Further, considering a scalar $z$ as $0 < z < (1/2)\lambda_{\min}(\mathbf{Q})$ one has

$$\dot{\bar{V}} \le -\{(1/2)\lambda_{\min}(\mathbf{Q}) - z\}||\boldsymbol{\xi}||^2 - z||\boldsymbol{\xi}||^2 + \varsigma. \tag{38}$$

The gains $\hat{\beta}_1, \hat{\beta}_2 \in \mathcal{L}_\infty$ in Case (i) and decrease in Case (ii). This implies $\exists \varpi \in \mathbb{R}^+$ such that $\sum_{j=0}^{1}(\hat{\beta}_j - \beta_j^*)^2/\gamma_j \le \varpi$. Therefore, the definition of $\bar{V}$ in (34) yields

$$\bar{V} \le \lambda_{\max}(\mathbf{P})||\boldsymbol{\xi}||^2 + \varpi. \tag{39}$$

Using the relation (39), (38) can be written as

$$\dot{\bar{V}} \le -\upsilon\bar{V} - z||\boldsymbol{\xi}||^2 + \varsigma + \upsilon\varpi, \tag{40}$$

where $\upsilon \triangleq (\frac{1}{2}\lambda_{\min}(\mathbf{Q}) - z)/\lambda_{\max}(\mathbf{P})$. Hence, $\dot{\bar{V}} < 0$ would be achieved when $||\boldsymbol{\xi}|| \ge \sqrt{(\varsigma + \upsilon\varpi)/z}$.

**Case (iii):** $||\mathbf{s}|| < \varphi$ and$\{$any $\hat{\beta}_j \le \underline{\beta}_j$ or $\mathbf{s}^T\dot{\mathbf{s}} > 0\}$
The fact $||\mathbf{s}|| < \epsilon$ implies that $\exists \bar{\epsilon} \in \mathbb{R}^+$ such that $||\boldsymbol{\xi}|| \le \bar{\epsilon}$ from the relation $\mathbf{s} = \mathbf{B}^T\mathbf{P}\boldsymbol{\xi}$. Using (14) we have

$$\begin{aligned} \dot{\bar{V}} &\le -(1/2)\boldsymbol{\xi}^T\mathbf{Q}\boldsymbol{\xi} + \mathbf{s}^T\{-\alpha c(\mathbf{s}/\sqrt{||\mathbf{s}||^2 + \epsilon}) + \boldsymbol{\sigma}\} \\ &\quad + ((\hat{\beta}_0 - \beta_0^*)/\gamma_0)\dot{\hat{\beta}}_0 + ((\hat{\beta}_1 - \beta_1^*)/\gamma_1)\dot{\hat{\beta}}_1 \\ &\le -(1/2)\lambda_{\min}(\mathbf{Q})||\boldsymbol{\xi}||^2 + (\hat{\beta}_0 + \hat{\beta}_1||\boldsymbol{\xi}||)||\mathbf{s}||. \end{aligned} \tag{41}$$

Unlike Case (i), proving boundedness of $\hat{\beta}_j$ in Case (iii) demands that $\hat{\beta}_j$s start decreasing in a finite time, i.e., $\mathbf{s}^T\dot{\mathbf{s}} \le 0$ should occur (from the second law of (33)) in a finite time. For this, we need to investigate only the evaluation of $V$, where gains only increase implying $\hat{\beta}_j > \underline{\beta}_j$. The condition $\mathbf{s}^T\dot{\mathbf{s}} > 0$ in Case (iii) implies $||\mathbf{s}||$ is increasing; thus $\exists \delta \in \mathbb{R}^+$ such that $||\mathbf{s}|| \ge \delta$. Further, using $||\mathbf{s}|| \le ||\mathbf{B}^T\mathbf{P}||||\boldsymbol{\xi}||$ we have

$$\delta \le ||\mathbf{s}|| \le ||\mathbf{B}^T\mathbf{P}||||\boldsymbol{\xi}|| \Rightarrow ||\boldsymbol{\xi}|| \ge \delta/||\mathbf{B}^T\mathbf{P}||. \tag{42}$$

Then, using (42), the adaptive law (33) yields

$$\dot{\hat{\beta}}_0 \geq \gamma_0\delta,\ \ \dot{\hat{\beta}}_1 \geq (\gamma_1\delta^2)/||\mathbf{B}^T\mathbf{P}||. \tag{43}$$

Using (33) and the fact $||\mathbf{s}|| < \varphi$ for Case (iii), the time derivative of $V(\boldsymbol{\xi}) = (1/2)\boldsymbol{\xi}^T\mathbf{P}\boldsymbol{\xi}$ for Case (iii) yields

$$\begin{aligned}\dot{V} &\leq -(1/2)\lambda_{\min}(\mathbf{Q})||\boldsymbol{\xi}||^2 + \mathbf{s}^T\{-\alpha c(\mathbf{s}/\sqrt{||\mathbf{s}||^2+\epsilon}) + \boldsymbol{\sigma}\}\\ &\leq -(\lambda_{\min}(\mathbf{Q})/\lambda_{\max}(\mathbf{P}))V + (\beta_0^* + \beta_1^*||\boldsymbol{\xi}||)||\mathbf{s}||\\ &\quad - \alpha(\hat{\beta}_0 + \hat{\beta}_1\|\boldsymbol{\xi}\|)(\delta||\mathbf{s}||/\sqrt{\varphi^2+\epsilon}).\end{aligned} \tag{44}$$

If $||\boldsymbol{\xi}||$ decreases, then it would also ensure that $||\mathbf{s}||$ decreases (i.e., $\mathbf{s}^T\dot{\mathbf{s}} < 0$) as $\mathbf{s} = \mathbf{B}^T\mathbf{P}\boldsymbol{\xi}$. Consequently, $\hat{\beta}_0, \hat{\beta}_1$ start decreasing following (33) and hence they would remain bounded individually. This feature can be realized if $\dot{V} < -\frac{\lambda_{\min}(\mathbf{Q})}{\lambda_{\max}(\mathbf{P})}V$ is established. Such condition can be achieved from (44) when

$$\alpha\hat{\beta}_0(\delta/\varrho) \geq \beta_0^*,\quad \alpha\hat{\beta}_1(\delta/\varrho) \geq \beta_1^*, \tag{45}$$

where $\varrho \triangleq \sqrt{\varphi^2+\epsilon}$. Since (43) defines the minimum rates of increments, (45) is satisfied within finite times $T_1, T_2$ where

$$T_1 \leq (\varrho\beta_0^*)/(\alpha\gamma_0\delta^2),\quad T_2 \leq (\varrho\beta_1^*||\mathbf{B}^T\mathbf{P}||)/(\alpha\gamma_1\delta^3). \tag{46}$$

Therefore, the exponential decrease of $||\boldsymbol{\xi}||$ and subsequent boundedness of $\hat{\beta}_j$ and $\hat{\beta}_1$ is achieved within a finite time $T = \max\{T_1\ T_2\}$. In addition, $||\mathbf{s}|| < \varphi$ in Case (iii) implies $||\boldsymbol{\xi}|| \in \mathcal{L}_\infty$ and consequently $(\hat{\beta}_0 + \hat{\beta}_1||\boldsymbol{\xi}||)||\mathbf{s}|| \leq \varpi_1$, where $\varpi_1 \in \mathbb{R}^+$. Using these results and the procedure in (40), the relation (41) can be written as

$$\dot{\bar{V}} \leq -\upsilon\bar{V} - z||\boldsymbol{\xi}||^2 + \varpi_1. \tag{47}$$

Hence, $\dot{\bar{V}} < 0$ would be established when $||\boldsymbol{\xi}|| \geq \sqrt{\varpi_1/z}$.

**Case (iv):** $||\mathbf{s}|| < \varphi$ and $\{\mathbf{s}^T\dot{\mathbf{s}} \leq 0$ and all $\hat{\beta}_j > \underline{\beta}_j\}$ Similarly, for this case

$$\begin{aligned}\dot{\bar{V}} &\leq -(1/2)\boldsymbol{\xi}^T\mathbf{Q}\boldsymbol{\xi} + \mathbf{s}^T\{-\alpha c(\mathbf{s}/\sqrt{||\mathbf{s}||^2+\epsilon}) + \boldsymbol{\sigma}\}\\ &\quad - ((\hat{\beta}_0 - \beta_0^*)/\gamma_0)\dot{\hat{\beta}}_0 - ((\hat{\beta}_1 - \beta_1^*)/\gamma_1)\dot{\hat{\beta}}_1\\ &\leq -(1/2)\lambda_{\min}(\mathbf{Q})||\boldsymbol{\xi}||^2 + 2(\beta_0^* + \beta_1^*||\boldsymbol{\xi}||)||\mathbf{s}||.\end{aligned} \tag{48}$$

This case can be analyzed exactly like Case (ii).

The stability results from Cases (i)-(iv) reveal that the closed-loop system is UUB. □

**Remark 5.** *Some recently proposed adaptive-robust TDC designs, namely [16], [23], [24], rely on the upper bound structure (10). Albeit conservativeness of (10), there is a crucial difference between an adaptive-robust design relying on (10) and one relying on (30): in the first case, one can leave the TDE error unattended (i.e., $\boldsymbol{\Delta}\mathbf{u} = \mathbf{0}$) and claim boundedness of the error dynamics; in the second case, this is impossible due to the explicit presence of $||\boldsymbol{\xi}||$ in the upper bound structure of $||\boldsymbol{\sigma}||$. Such a fundamental difference leads to a completely different and more challenging design and stability analysis which, to the best of the authors' knowledge, has been missing in the existing literature.*

**Selection of Various Design Parameters:** As (1) is a second-order dynamics, the gains $\mathbf{K}_P, \mathbf{K}_D$ are usually selected as $\mathbf{K}_P = \omega_n^2\mathbf{I}$ and $\mathbf{K}_D = 2\zeta\omega_n\mathbf{I}$, where $\omega_n$ and $\zeta$ are the desired natural frequency and damping ratio, respectively, for the unperturbed (or nominal) error dynamics [13], [19], [20]. The scalar $\gamma_j > 0$ is designed to tune the rate of change in $\hat{\beta}_j$ in (33), which is to be selected as per applications.

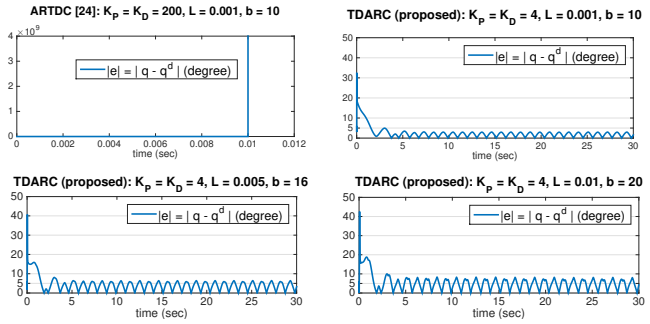


Fig. 2. Tracking performance of TDARC and ARTDC [24] for system (12).

## V. Verification of the Proposed TDARC

To judge its effectiveness, the proposed TDARC scheme is compared with adaptive-robust TDC of [24] (called ARTDC henceforth), having adaptive law for switching gain $c$ (cf. (14))

$$\dot{c} = \begin{cases}\gamma_0||\mathbf{s}||, & \text{if } c \leq \underline{\beta}_0 \text{ or } (||\mathbf{s}|| - ||\mathbf{s}_L||) > 0\\ -\gamma_0||\mathbf{s}||, & \text{if } (||\mathbf{s}|| - ||\mathbf{s}_L||) \leq 0\end{cases}. \tag{49}$$

### A. Simulation Results and Analysis

We apply the proposed TDARC and ARTDC [24] to (12) to check whether they can successfully track the desired trajectory while conventional TDC failed. The following parameters are selected for parity: $\gamma_0 = \gamma_1 = 20, \epsilon = 0.1, \alpha = 1$, $\hat{\beta}_0(0) = \hat{\beta}_1(0) = c(0) = 0.01, \underline{\beta}_0 = \underline{\beta}_1 = 0.0001$. Fig. 2 reveals that ARTDC [24] cannot stabilize the system even with large $K_P = K_D = 200$, whereas, with the same $L$, TDARC succeeds with much lower $K_P = K_D = 4$. This confirms the importance of the proposed state-dependent structure as in (30). Further, Fig. 2 shows that TDARC is robust against large values of $L$ and $b$, whereas conventional TDC has shown instability (scenarios (iv) and (v) in Fig. 1).

### B. Experimental Results and Analysis

In this subsection, performance of the proposed TDARC is verified experimentally against conventional TDC [2] and ARTDC [24] on a biped robot setup, named cCub [30] (Fig. 3). The robot weighs 18.3 kg, and is 0.676 m tall from feet to hip roll joint axes. Each leg of cCub has six degrees-of-freedom (DoFs). For experimental purposes, the robot is treated as a manipulator with dynamics as in (1), where the three pitch joints (in the sagittal plane) hip ($q_1$), knee ($q_2$) and ankle joints ($q_3$) are controlled while other joints are kept fixed at zero angles. Thus, six joints are operated simultaneously for both legs. Each joint is torque-controlled by an embedded micro-controller. The realtime control system is implemented in Simulink Real-Time™ which communicates with the robot through Ethernet connection with a sampling rate of 1 kHz, i.e., $L$ = 0.001 is set in the controllers.

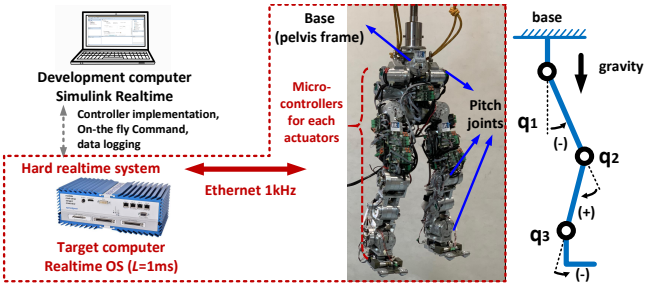


Fig. 3. The experimental setup of the cCub robot: the hard realtime control system with sampling time $L$=1 ms and the schematic diagram.

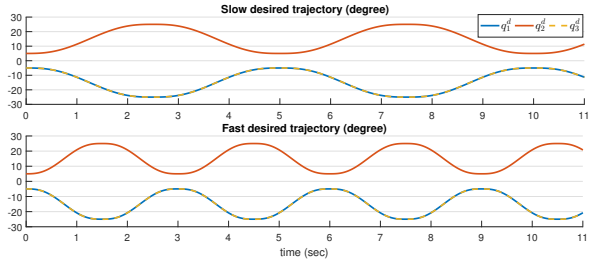


Fig. 4. Desired trajectories for the three pitch joints.

To properly judge the performance of the proposed controller, two experimental scenarios, S1 and S2, are considered in following subsections. For both S1 and S2, the control design parameters are: $\bar{\mathbf{M}} = 0.037\mathbf{I}$ (kgm$^2$), $\mathbf{K}_P = 144\mathbf{I}$, $\mathbf{K}_D = 24\mathbf{I}$, $\mathbf{Q} = \mathbf{I}$, $\epsilon = 5 \times 10^{-5}$, $\alpha = 4, \gamma_j = 1, \underline{\beta}_j = 0$, $\hat{\beta}_j(0) = 0$, $j = 0, 1$. For parity in the comparison, same values of $\bar{\mathbf{M}}, \mathbf{K}_P, \mathbf{K}_D$ and $\alpha, \gamma_0, \underline{\beta}_0$ are selected for the conventional TDC (5)-(7) and ARTDC (49).

Due to symmetry in the mechanical structure of cCub robot, we only present the results for the right leg to avoid repetition.

*1) Description of Scenario S1:* In this scenario we test the capability of TDC [2], ARTDC [24] and the proposed TDARC to adapt to changes in the desired trajectory. To this purpose, two periodic desired trajectories having different speeds are selected as in Fig. 4. For simplicity, no external disturbances are considered in this scenario by keeping the robot hung in the air, that is, no ground contact was made.

*Results and Discussion for S1:* The tracking performance of TDC, ARTDC and TDARC are demonstrated in Fig. 5a - 5b, while the control input and evolution of various switching gains for TDARC and ARTDC are depicted in Figs. 6a-6b and in Figs. 7a-7b for the slower and fast desired trajectories, respectively. The controllers' performances are collected in Table I in terms of root mean squared (RMS) error, maximum absolute error (MAE) and RMS $\boldsymbol{\tau}$.

Table I reveals that TDARC provides minimum performance improvements of 53.7% (resp. 62.2%) and 34.3% (resp. 16.7%) in RMSE and of 28.5% (resp. 33.7%) and 21.2% (resp. 24.1%) in MAE for the slower (resp. fast) trajectory as compared to TDC and ARTDC respectively across all the joints. Remarkably, this is achieved with less control effort compared to ARTDC. These results clearly demonstrate the importance/effectiveness of the proposed TDARC scheme over the conventional TDC and ARTDC [24].

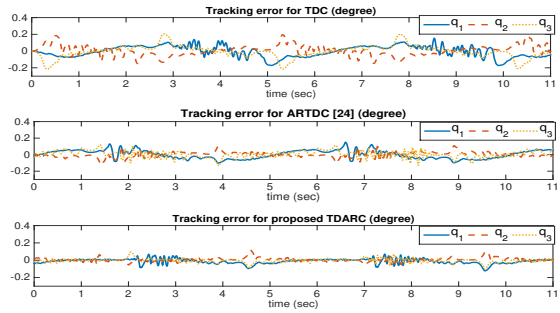


(a) for the slower trajectory

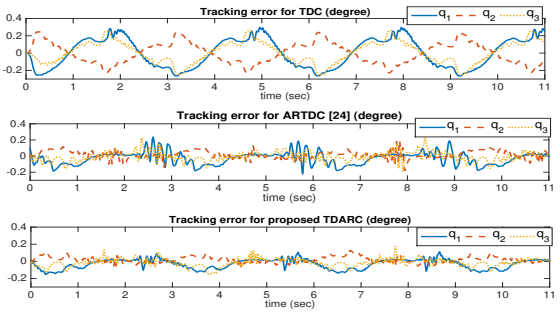


(b) for the fast trajectory

Fig. 5. Performance comparison between TDC, ARTDC [24] and TDARC.

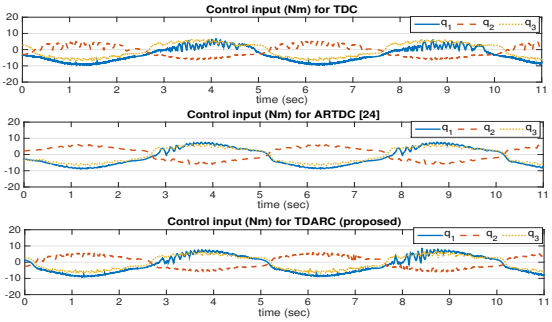


(a) for the slower trajectory

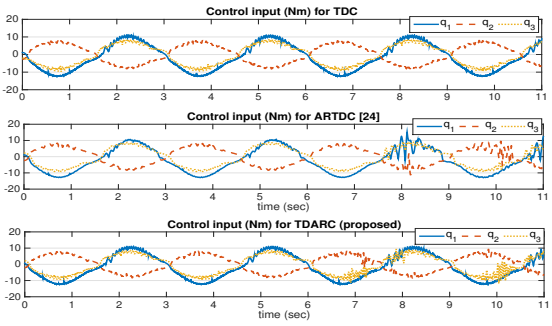


(b) for the fast trajectory

Fig. 6. Control input comparison between TDC, ARTDC [24] and TDARC.

*2) Description of Scenario S2:* This scenario extensively verifies the robustness property of TDARC in the presence of dynamic external disturbances, while following the slower desired trajectory shown in Fig. 4. This scenario is designed as a combination of five phases (cf. Fig. 8), elaborated as follows:

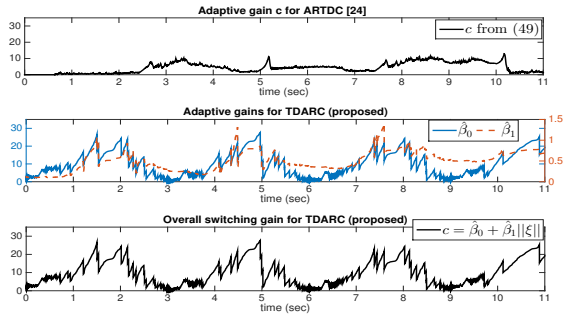


(a) for the slower trajectory

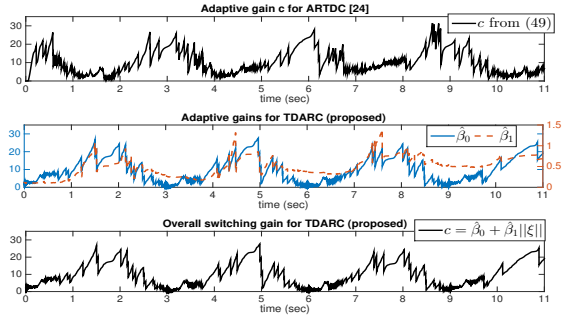


(b) for the fast trajectory

Fig. 7. Evolution of various switching gains for TDARC and ARTDC [24].

TABLE I
PERFORMANCE COMPARISON FOR SCENARIO S1

| Joints | RMS error (degree) | | | | | |
|---|---|---|---|---|---|---|
| | Slower Trajectory | | | Fast Trajectory | | |
| | TDC | ARTDC | **TDARC** | TDC | ARTDC | **TDARC** |
| $q_1$ | 0.067 | 0.053 | **0.031** | 0.167 | 0.080 | **0.063** |
| $q_2$ | 0.062 | 0.035 | **0.023** | 0.119 | 0.051 | **0.039** |
| $q_3$ | 0.075 | 0.043 | **0.022** | 0.126 | 0.056 | **0.047** |
| | MAE (degree) | | | | | |
| $q_1$ | 0.172 | 0.156 | **0.123** | 0.295 | 0.234 | **0.153** |
| $q_2$ | 0.196 | 0.144 | **0.113** | 0.246 | 0.190 | **0.136** |
| $q_3$ | 0.217 | 0.133 | **0.102** | 0.261 | 0.228 | **0.173** |
| | RMS $\tau$ (Nm) | | | | | |
| $q_1$ | 5.351 | 5.488 | **5.281** | 7.291 | 7.773 | **7.634** |
| $q_2$ | 3.697 | 4.014 | **3.955** | 5.316 | 5.365 | **5.103** |
| $q_3$ | 4.325 | 4.437 | **4.348** | 5.778 | 5.781 | **5.578** |

(i) In Phase 1 ($t$=0-20s), the robot was kept hung in the air.
(ii) In Phase 2 ($t$=20-36s), the robot was placed on the ground at approximately $t$=20s while it was still following the desired trajectory (*now a squat like motion on the ground*). In this phase, the ground reaction force is exerted on the robot and gets propagated throughout its body, acting as a highly nonlinear external disturbance.
(iii) In Phase 3 ($t$=36-50s), an additional payload of 3.3kg (18% of cCub's weight) was suddenly added on the pelvis of the robot at approximately $t$=36s and kept during this entire phase, while the robot was performing the squat motion. Therefore, in Phase 3, two different disturbances namely, ground reaction forces and the additional payload are applied simultaneously.
(iv) During Phase 4 ($t$=50-67s), the payload was quickly removed at approximately $t$=50s leading to radical changes of the disturbance. Hence, ground reaction force was the only source of external disturbance for this phase.
(v) Lastly, in Phase 5 (after $t$=67s), the robot was again pulled away from the ground and thereby, the ground reaction force was suddenly eliminated around $t$=67s.

TABLE II
TRACKING PERFORMANCE OF TDARC FOR S2

| Joints | RMS error (degree) | | | | |
|---|---|---|---|---|---|
| | Phase 1 | Phase 2 | Phase 3 | Phase 4 | Phase 5 |
| $q_1$ | 0.029 | 0.043 | 0.037 | 0.042 | 0.031 |
| $q_2$ | 0.021 | 0.032 | 0.034 | 0.033 | 0.021 |
| $q_3$ | 0.027 | 0.035 | 0.029 | 0.032 | 0.026 |
| | MAE (degree) | | | | |
| $q_1$ | 0.117 | 0.139 | 0.108 | 0.141 | 0.122 |
| $q_2$ | 0.116 | 0.129 | 0.124 | 0.134 | 0.085 |
| $q_3$ | 0.141 | 0.134 | 0.122 | 0.106 | 0.115 |
| | RMS $\tau$ (Nm) | | | | |
| $q_1$ | 5.178 | 4.503 | 5.211 | 4.574 | 5.266 |
| $q_2$ | 3.988 | 4.605 | 4.284 | 4.474 | 4.003 |
| $q_3$ | 4.416 | 4.041 | 5.032 | 4.229 | 4.200 |

*Results and Discussion for S2:* The tracking performance of TDARC for this scenario is demonstrated via Figs. 9, 10 and Table II: these results reveal that the performance of TDARC is uniform throughout this scenario, i.e., tracking results of Phases 1 and 5, and Phases 2 and 4 are almost similar under the same nature of disturbances. Interestingly, upon comparing Tables I and II, it can be observed that for the same desired trajectory, TDARC under influences of considerable disturbances (Phases 2, 3 and 4 in S2) still outperforms TDC and ARTDC without any external disturbances (i.e. in S1).

## VI. CONCLUSION

In this paper, various conservative aspects of the conventional TDC was analytically proved and mitigated. Specifically, a new state-dependent upper bound structure for the TDE error was introduced avoiding any a priori bounded assumption of TDE error. The proposed structure highlighted the need for a new design philosophy, as the closed-loop system stability cannot be ensured unless the TDE error is dealt. Consequently, a new adaptive-robust design, TDARC, was formulated to compensate for the TDE error. Extensive simulations and experiments verified the effectiveness of the proposed TDARC compared to conventional TDC schemes. A future work would be to explore higher order sliding mode [31], [32] to avoid boundary layer.

## REFERENCES

[1] T. Hsia and L. Gao, "Robot manipulator control using decentralized linear time-invariant time-delayed joint controllers," in *proc. IEEE Int. Conf. Robot. Autom.* IEEE, 1990, pp. 2070–2075.
[2] T. S. Hsia, T. Lasky, and Z. Guo, "Robust independent joint controller design for industrial robot manipulators," *IEEE Trans. Ind. Electron.*, vol. 38, no. 1, pp. 21–25, 1991.
[3] K. Youcef-Toumi and O. Ito, "A time delay controller for systems with unknown dynamics," *ASME J. Dyn. Syst. Meas. Control*, vol. 112, no. 1, pp. 133–142, 1990.
[4] S. Roy, S. Nandy, R. Ray, and S. N. Shome, "Robust path tracking control of nonholonomic wheeled mobile robot: Experimental validation," *Int. J. Control Autom. Syst.*, vol. 13, no. 4, pp. 897–905, 2015.

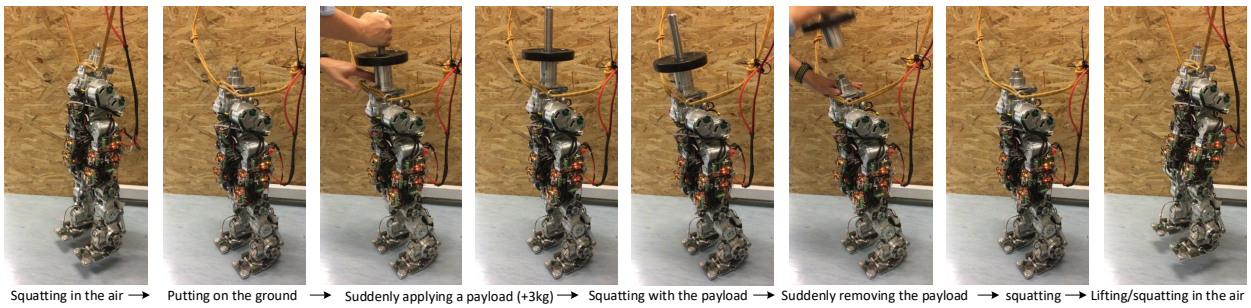


Fig. 8. The snapshots of the experiment in S2, where significant external disturbances are applied and radically changed.

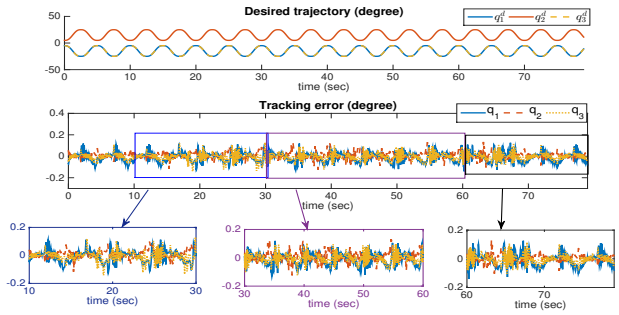


Fig. 9. Robust tracking performance of TDARC for S2.

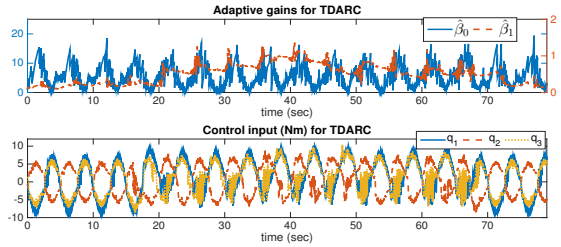


Fig. 10. Evolution of switching gains and control input of TDARC for S2.


[5] J. Lee et al., "An experimental study on time delay control of actuation system of tilt rotor unmanned aerial vehicle," *Mechatron.*, vol. 22, no. 2, pp. 184–194, 2012.

[6] S. Roy and I. N. Kar, "Adaptive-robust control of uncertain euler-lagrange systems with past data: A time-delayed approach," in *proc. IEEE Int. Conf. Robot. Autom.* IEEE, 2016, pp. 5715–5720.

[7] J. Kim et al., "Time-delay controller design for position control of autonomous underwater vehicle under disturbances," *IEEE Trans. Ind. Electron.*, vol. 63, no. 2, pp. 1052–1061, 2016.

[8] M. Jin, J. Lee, and K. K. Ahn, "Continuous nonsingular terminal sliding-mode control of shape memory alloy actuators using time delay estimation," *IEEE/ASME Trans. Mechatron.*, vol. 20, no. 2, pp. 899–909, 2015.

[9] H. J. Lee and J. J. Lee, "Time delay control of a shape memory alloy actuator," *Smart Mater. Struct.*, vol. 13, no. 1, p. 227, 2004.

[10] S.-M. Chin, C.-O. Lee, and P. H. Chang, "An experimental study on the position control of an electrohydraulic servo system using time delay control," *Control Eng. Pract.*, vol. 2, no. 1, pp. 41–48, 1994.

[11] J. H. Lee et al., "Time-delay control of ionic polymer metal composite actuator," *Smart Mater. Struct.*, vol. 24, no. 4, p. 047002, 2015.

[12] P. Chang, D. Kim, and K. Park, "Robust force/position control of a robot manipulator using time-delay control," *Control Eng. Pract.*, vol. 3, no. 9, pp. 1255–1264, 1995.

[13] M. Jin, S. H. Kang, and P. H. Chang, "Robust compliant motion control of robot with nonlinear friction using time-delay estimation," *IEEE Trans. Ind. Electron.*, vol. 55, no. 1, pp. 258–269, 2008.

[14] M. Jin, J. Lee, P. H. Chang, and C. Choi, "Practical nonsingular terminal sliding-mode control of robot manipulators for high-accuracy tracking control," *IEEE Trans. Ind. Electron.*, vol. 56, no. 9, pp. 3593–3601, 2009.

[15] J. Lee, H. Dallali, M. Jin, D. G. Caldwell, and N. G. Tsagarakis, "Robust and adaptive dynamic controller for fully-actuated robots in operational space under uncertainties," *Autonomous Robots*, vol. 43, no. 4, pp. 1023–1040, 2019.

[16] M. Jin, J. Lee, and N. G. Tsagarakis, "Model-free robust adaptive control of humanoid robots with flexible joints," *IEEE Trans. Ind. Electron.*, vol. 64, no. 2, pp. 1706–1715, 2017.

[17] Y.-B. Kim, "Improving dynamic performance of proton-exchange membrane fuel cell system using time delay control," *J. Power Sources*, vol. 195, no. 19, pp. 6329–6341, 2010.

[18] K.-H. Kim and M.-J. Youn, "A simple and robust digital current control technique of a PM synchronous motor using time delay control approach," *IEEE Trans. Power Electron.*, vol. 16, no. 1, pp. 72–82, 2001.

[19] G. R. Cho, P. H. Chang, S. H. Park, and M. Jin, "Robust tracking under nonlinear friction using time-delay control with internal model," *IEEE Trans. Control Syst. Technol.*, vol. 17, no. 6, pp. 1406–1414, 2009.

[20] J. Lee, P. H. Chang, and R. S. Jamisola, "Relative impedance control for dual-arm robots performing asymmetric bimanual tasks," *IEEE Trans. Ind. Electron.*, vol. 61, no. 7, pp. 3786–3796, 2014.

[21] D. K. Han and P.-h. Chang, "Robust tracking of robot manipulator with nonlinear friction using time delay control with gradient estimator," *J. Mech. Sci. Technol.*, vol. 24, no. 8, pp. 1743–1752, 2010.

[22] S. Roy, S. Nandy, R. Ray, and S. N. Shome, "Time delay sliding mode control of nonholonomic wheeled mobile robot: experimental validation," in *proc. IEEE Int. Conf. Robot. Autom.* IEEE, 2014, pp. 2886–2892.

[23] J. Baek, M. Jin, and S. Han, "A new adaptive sliding-mode control scheme for application to robot manipulators," *IEEE Trans. Ind. Electron.*, vol. 63, no. 6, pp. 3628–3637, 2016.

[24] S. Roy, I. N. Kar, J. Lee, N. G. Tsagarakis, and D. G. Caldwell, "Adaptive-robust control of a class of EL systems with parametric variations using artificially delayed input and position feedback," *IEEE Trans. Control Syst. Technol.*, vol. 27, no. 2, pp. 603–615, 2019.

[25] M. W. Spong, S. Hutchinson, and M. Vidyasagar, *Robot dynamics and control*. John Wiley & Sons, 2008.

[26] S. Roy, S. Baldi, and L. M. Fridman, "On adaptive sliding mode control without a priori bounded uncertainty," *Automatica*, vol. 111, p. 108650, 2020.

[27] S. Roy, S. B. Roy, J. Lee, and S. Baldi, "Overcoming the underestimation and overestimation problems in adaptive sliding mode control," *IEEE/ASME Trans. Mechatron.*, vol. 24, no. 5, pp. 2031–2039, 2019.

[28] W. Rudin *et al.*, *Principles of mathematical analysis*. McGraw-Hill New York, 1964, vol. 3.

[29] J. Baek, W. Kwon, B. Kim, and S. Han, "A widely adaptive time-delayed control and its application to robot manipulators," *IEEE Trans. Indus. Electron.*, vol. 66, no. 7, pp. 5332–5342, 2019.

[30] N. G. Tsagarakis, Z. Li, J. Saglia, and D. G. Caldwell, "The design of the lower body of the compliant humanoid robot cCub," in *proc. IEEE Int. Conf. Robot. Autom.* IEEE, 2011, pp. 2035–2040.

[31] S. Mobayen and F. Tchier, "A novel robust adaptive second-order sliding mode tracking control technique for uncertain dynamical systems with matched and unmatched disturbances," *Int. J. Control Autom. Syst.*, vol. 15, no. 3, pp. 1097–1106, 2017.

[32] D. A. Haghighi and S. Mobayen, "Design of an adaptive super-twisting decoupled terminal sliding mode control scheme for a class of fourth-order systems," *ISA Trans.*, vol. 75, pp. 216–225, 2018.